The Vibrational Analysis of Cyclopentanone[1]

V. B. KARTHA,[2] H. H. MANTSCH,[3] AND R. N. JONES
Division of Chemistry, National Research Council of Canada, Ottawa, Canada K1A 0R6

Received May 2, 1972[4]

The infrared and Raman spectra of cyclopentanone, ααα′α′-d_4-cyclopentanone, βββ′β′-d_4-cyclopentanone and d_8-cyclopentanone have been measured and a normal co-ordinate analysis performed based on a twisted C_2 conformation. The 36 normal vibrations were computed using a selective valence force field comprising 16 diagonal and 16 off-diagonal force constants. The 4 isotopic species provided 144 frequencies to refine 15 diagonal force constants. The initial values of the constants were transferred from a force field for cyclohexanone computed in this laboratory. The infrared and Raman spectra were analyzed in terms of the potential energy distribution coefficients categorized as group frequencies, zone frequencies, and delocalized frequencies.

Les spectres infrarouge et Raman de la cyclopentanone, de la cyclopentanone ααα′α′-d_4, de la cyclopentanone βββ′β′-d_4 et de la cyclopentanone-d_8 ont été étudiés et une analyse (en coordonnées normales) a été effectuée en se basant sur une conformation C_2 croisée. Les 36 vibrations normales ont été evaluées en utilisant un champ de force valentielle sélectif qui comprend 16 constantes de force diagonales et 16 autres non-diagonales. Les 4 espèces isotopiques ont engendré 144 fréquences qui ont aidé à déterminer 15 constantes de force diagonales. Les valeurs initiales des constantes ont été obtenues d'un champ de force pour la cyclohexanone calculé dans ce laboratoire. Les spectres infrarouge et Raman ont été analysés en fonction des coefficients de distribution d'énergie potentielle classés selon des fréquences de groupe, des fréquences de zone et des fréquences délocalisées.

[Traduit par le journal]

Can. J. Chem., 51, 1749 (1973)

Introduction

This paper is concerned with a vibrational analysis of cyclopentanone and three deuterium substituted species (**1**–**4**); it supplements earlier work on cyclohexanone (1). These studies are being made to assess the capabilities and limitations of a simplified normal co-ordinate treatment to aid in the interpretation of the vibrational spectra of molecules of low symmetry related to natural products with particular reference to steroids.

Several conformations varying from planar (C_{2v}) to lower symmetries (C_2, C_s, C_1) have been

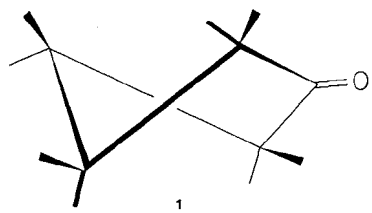

1

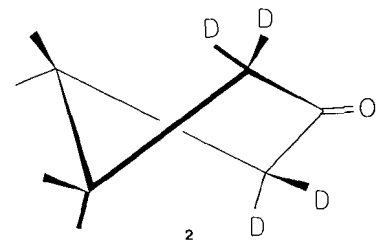

2

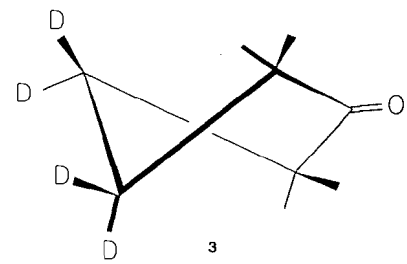

3

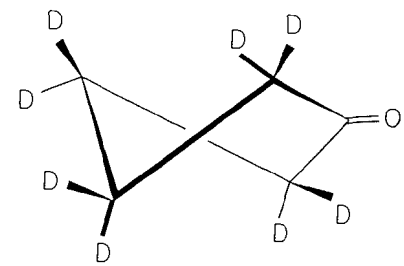

4

[1]NRCC No. 13046. Presented in part at a joint session of the Physical Chemistry and Organic Chemistry Divisions of the Chemical Institute of Canada, Halifax, Nova Scotia, May 1971.

[2]NRCC Postdoctorate Fellow, 1967–1969.

[3]NRCC Postdoctorate Fellow, 1969–1971.

[4]Revision received December 29, 1972.

proposed for cyclopentanone; they have been reviewed by Howard-Lock and King (2). The ground state geometry assumed in this work (Fig. 1) is based on a least squares fit of the bond parameters (Table 1) to the rotational constants of **1**, **2**, **4**, and two conformers of α-*d*-cyclopentanone (**5**, **6**). The rotational constants were taken from microwave data in the literature (3–7). Calculations were performed with the twisted C_2 and the bent C_3 structures.[5] All 9 parameters were allowed to adjust until the sum of the squares of the differences between the reported and computed rotational constants was minimal. The only restraint was that the C_2—C_3 and C_3—C_4 bond

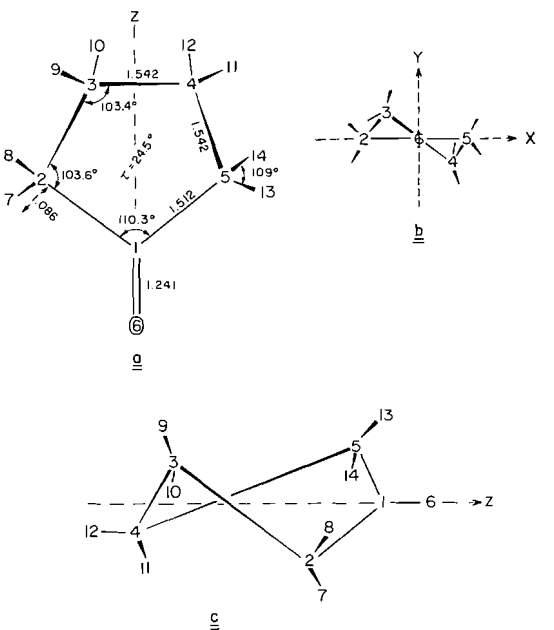

FIG. 1. Atom numeration and geometric parameters in the skew configuration.

TABLE 1. Molecular parameters for cyclopentanone derived from microwave measurements

No.	Parameter	Refined value
1	C_1—C_2	1.512 Å
2	C_2—C_3; C_3—C_4	1.542 Å
3	C=O	1.241 Å
4	C—H	1.086 Å
5	∠ $C_5C_1C_2$	110.283°
6	∠ $C_1C_2C_3$	103.576°
7	∠ $C_2C_3C_4$	103.443°
8	∠ HCH	108.999°
9	Twist angle	24.519°

[5]See Fig. 2 of ref. 2.

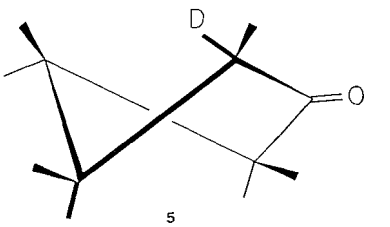

5

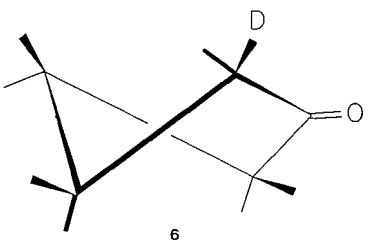

6

lengths remained equal and the calculations were considered self-consistant when the variations in the bond lengths were less than 0.001 Å.[6] The C_2 conformation in which the ring is twisted in a skew configuration gave much the better fit. Such a C_2 ground state is consistent with similar calculations[7] of Kim and Gwinn (7) and Howard-Lock and King (2) and with more recent far infrared studies of Ikeda and Lord (8), and electron diffraction measurements of Geise and Mijlhoff (9).

The Cartesian co-ordinates of the equilibrium positions of the atoms were computed with respect to an origin centered at the mid-point of the C_2—C_5 axis (Table 2). The 47 selected internal valance co-ordinates are identified[8] in Figs. 2 and 3. Under C_2 symmetry the 36 normal vibrations divide into 18 type A (Raman polarized) and 18 type B (Raman depolarized), and all are infrared and Raman active. The 47 internal co-ordinates were combined into 47 non-normalized symmetry co-ordinates (Table 3). As there are 36 normal modes 11 symmetry co-ordinates are redundant. The local redun-

[6]All molecular dimensions are reported in Å (1 Å = 10^{-10} m).

[7]The refined bond parameters in Table 1 differ slightly from those reported in refs. 2 and 7. Our twist angle (24.5°) is close to that of Kim and Gwinn (24°) but Howard-Lock and King obtained 33°. Our differences from Kim and Gwinn's bond lengths are probably due to the fact that they held the C—H and C=O bond lengths and the CH_2 angles fixed during refinement while we allowed them to adjust.

[8]Figure 1 exhibits the true projections of the non-planar ring but the projection diagrams appearing elsewhere have been distorted to permit more space to portray the bond and angle motions within the ring.

TABLE 2. Cartesian co-ordinates of cyclopentanone in the C_2 skew conformation

Atom No.*	Co-ordinates (Å)	Atom No.	Co-ordinates (Å)
1(C)	$x = 0.0$, $y = 0.0$, $z = 0.864448$	8(H)	$x = -1.945792$, $y = 0.758048$, $z = 0.329162$
2(C)	$x = -1.241065$, $y = 0.0$, $z = 0.0$	9(H)	$x = -0.641546$, $y = 1.392274$, $z = -1.569303$
3(C)	$x = -0.701264$, $y = 0.319867$, $z = -1.408063$	10(H)	$x = -1.330775$, $y = -0.118765$, $z = -2.176788$
4(C)	$x = 0.701264$, $y = -0.319867$, $z = -1.408063$	11(H)	$x = 0.641546$, $y = -1.392274$, $z = -1.569303$
5(C)	$x = 1.241065$, $y = 0.0$, $z = 0.0$	12(H)	$x = 1.330775$, $y = 0.118765$, $z = -2.176788$
6(O)	$x = 0.0$, $y = 0.0$, $z = 2.105452$	13(H)	$x = 1.730035$, $y = 0.969616$, $z = 0.019405$
7(H)	$x = -1.730035$, $y = -0.969616$, $z = 0.019405$	14(H)	$x = 1.945792$, $y = -0.758048$, $z = 0.329162$

*For numbering of atoms see Fig. 1.

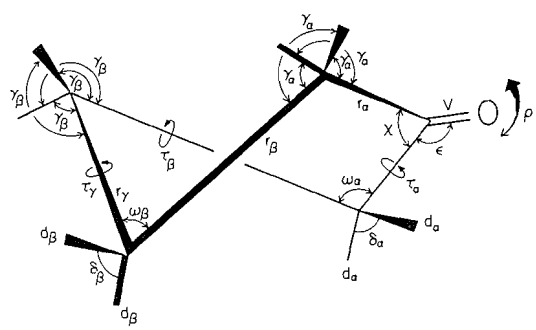

FIG. 2. Internal valence co-ordinates.

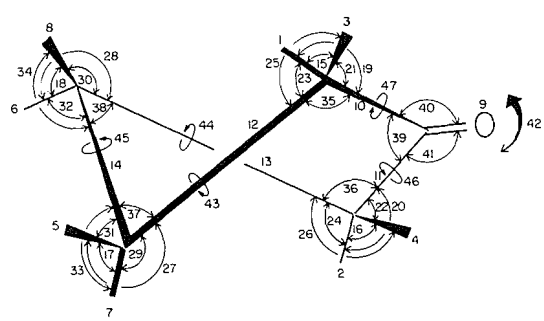

FIG. 3. Numerical identification of the internal valence co-ordinates.

dancies at the 5 carbon atoms are easily recognized and the remaining 6 are eliminated during normalization by the GMAT program (1, 10).

Experimental

1 and **4** are commercially available compounds while **2** and **3** were prepared by exchange reactions at the active α positions.

Cyclopentanone (1)

An Eastman Organic Chemical reagent grade sample was distilled under reduced pressure in a Nester–Faust spinning band column.

αα′α′-d_4-Cyclopentanone (2)

Cyclopentanone (30 ml), purified as above, was stirred with D_2O (99.7%, 60 ml) and Na_2CO_3 (600 mg) at room temperature for 24 h in a sealed glass tube. The product was extracted with ether, dried ($MgSO_4$), the ether removed, and the residue distilled under reduced pressure (55–60 Torr). The product was twice recycled under the same conditions. In the final distillation the first fraction (3.5 ml) was discarded and the next 5 ml collected. The infrared spectrum showed negligible H_2O or D_2O absorption and indicated almost complete α-deuteration. Mass spectrum analysis, when extrapolated to zero ionization voltage, indicate a d_4 content in excess of 90%.

ββββ′β′-d_8-Cyclopentanone (3)

d_8-Cyclopentanone (1 ml) was stirred with H_2O (3 ml) and Na_2CO_3 (30 mg) in an all-glass system for 24 h at room temperature. The product was extracted with ether, the ether removed by evaporation at room temperature, and the residue again treated for 24 h with H_2O (2 ml)

TABLE 3. Symmetry co-ordinates of cyclopentanone in the C_2 skew configuration (not normalized)

Internal co-ordinates involved*	Approximate description†
Type A	
$S_1 = d_1+d_2-d_3-d_4$	asym α CH stretch
$S_2 = d_5+d_6-d_7-d_8$	asym β CH stretch
$S_3 = d_1+d_2+d_3+d_4$	sym α CH stretch
$S_4 = d_5+d_6+d_7+d_8$	sym β CH stretch
$S_5 = v_9$	C=O stretch
$S_6 = r_{10}+r_{11}$	α C—C stretch
$S_7 = r_{12}+r_{13}$	β C—C stretch
$S_8 = r_{14}$	γ C—C stretch
$S_9 = \delta_{15}+\delta_{16}$	α CH_2 scissor
$S_{10} = \delta_{17}+\delta_{18}$	β CH_2 scissor
$S_{11} = \gamma_{19}+\gamma_{20}+\gamma_{21}+\gamma_{22}-\gamma_{23}-\gamma_{24}-\gamma_{25}-\gamma_{26}$	α CH_2 wag
$S_{12} = \gamma_{27}+\gamma_{28}+\gamma_{29}+\gamma_{30}-\gamma_{31}-\gamma_{32}-\gamma_{33}-\gamma_{34}$	β CH_2 wag
$S_{13} = \gamma_{19}+\gamma_{20}-\gamma_{21}-\gamma_{22}-\gamma_{23}-\gamma_{24}+\gamma_{25}+\gamma_{26}$	α CH_2 twist
$S_{14} = \gamma_{27}+\gamma_{28}-\gamma_{29}-\gamma_{30}-\gamma_{31}-\gamma_{32}+\gamma_{33}+\gamma_{34}$	β CH_2 twist
$S_{15} = \gamma_{19}+\gamma_{20}-\gamma_{21}-\gamma_{22}+\gamma_{23}+\gamma_{24}-\gamma_{25}-\gamma_{26}$	α CH_2 rock
$S_{16} = \gamma_{27}+\gamma_{28}-\gamma_{29}-\gamma_{30}+\gamma_{31}+\gamma_{32}-\gamma_{33}-\gamma_{34}$	β CH_2 rock
$S_{17} = \gamma_{19}+\gamma_{20}+\gamma_{21}+\gamma_{22}+\gamma_{23}+\gamma_{24}+\gamma_{25}+\gamma_{26}$	Redundant
$S_{18} = \gamma_{27}+\gamma_{28}+\gamma_{29}+\gamma_{30}+\gamma_{31}+\gamma_{32}+\gamma_{33}+\gamma_{34}$	Redundant
$S_{19} = \omega_{35}+\omega_{36}$	α-CCC bend
$S_{20} = \omega_{37}+\omega_{38}$	β-CCC bend
$S_{21} = \chi_{39}-\varepsilon_{40}-\varepsilon_{41}$	C_α—CO—C_α bend
$S_{22} = \chi_{39}+\varepsilon_{40}+\varepsilon_{41}$	Redundant
$S_{23} = \tau_{43}+\tau_{44}$	$C_\alpha C_\beta$ torsion
$S_{24} = \tau_{45}$	$C_\beta C_\beta$ torsion
$S_{25} = \tau_{46}+\tau_{47}$	C_αC(O) torsion
Type B	
$S_{26} = d_1-d_2-d_3+d_4$	asym α CH stretch
$S_{27} = d_5-d_6-d_7+d_8$	asym β CH stretch
$S_{28} = d_1-d_2+d_3-d_4$	sym α CH stretch
$S_{29} = d_5-d_6+d_7-d_8$	sym β CH stretch
$S_{30} = r_{10}-r_{11}$	α C—C stretch
$S_{31} = -r_{12}+r_{13}$	β C—C stretch
$S_{32} = \delta_{15}-\delta_{16}$	α CH_2 scissor
$S_{33} = \delta_{17}-\delta_{18}$	β CH_2 scissor
$S_{34} = \gamma_{19}-\gamma_{20}+\gamma_{21}-\gamma_{22}-\gamma_{23}+\gamma_{24}-\gamma_{25}+\gamma_{26}$	α CH_2 wag
$S_{35} = \gamma_{27}-\gamma_{28}+\gamma_{29}-\gamma_{30}-\gamma_{31}+\gamma_{32}-\gamma_{33}+\gamma_{34}$	β CH_2 wag
$S_{36} = \gamma_{19}-\gamma_{20}-\gamma_{21}+\gamma_{22}-\gamma_{23}+\gamma_{24}+\gamma_{25}-\gamma_{26}$	α CH_2 twist
$S_{37} = \gamma_{27}-\gamma_{28}-\gamma_{29}+\gamma_{30}-\gamma_{31}+\gamma_{32}+\gamma_{33}-\gamma_{34}$	β CH_2 twist
$S_{38} = \gamma_{19}-\gamma_{20}-\gamma_{21}+\gamma_{22}+\gamma_{23}-\gamma_{24}-\gamma_{25}+\gamma_{26}$	α CH_2 rock
$S_{39} = \gamma_{27}-\gamma_{28}-\gamma_{29}+\gamma_{30}+\gamma_{31}-\gamma_{32}-\gamma_{33}+\gamma_{34}$	β CH_2 rock
$S_{40} = \gamma_{19}-\gamma_{20}+\gamma_{21}-\gamma_{22}+\gamma_{23}-\gamma_{24}+\gamma_{25}-\gamma_{26}$	Redundant
$S_{41} = \gamma_{27}-\gamma_{28}+\gamma_{29}-\gamma_{30}+\gamma_{31}-\gamma_{32}+\gamma_{33}-\gamma_{34}$	Redundant
$S_{42} = \omega_{35}-\omega_{36}$	α CCC bend
$S_{43} = -\omega_{37}+\omega_{38}$	β CCC bend
$S_{44} = \varepsilon_{40}-\varepsilon_{41}$	C=O bend in-plane
$S_{45} = \rho_{42}$	C=O bend out-of-plane
$S_{46} = \tau_{43}-\tau_{44}$	$C_\alpha C_\beta$ torsion
$S_{47} = \tau_{46}-\tau_{47}$	C_αC(O) torsion

*The + and − signs respectively identify an increase or decrease of the bond length or bond angle during the vibration.

†All symmetry co-ordinates involving combinations of symmetric internal co-ordinates yield in-phase (Type A) and out-of-phase (Type B) vibrations for which the same description is used. Asym (antisymmetric) and sym (symmetric) refer to the local site symmetry not to the symmetry axis of the molecule.

and Na_2CO_3 (200 mg). The product was extracted three times with 4 ml portions of ether and the bulked extracts dried with freshly regenerated molecular sieve type 4A. The ether was removed by distillation and the residue distilled under reduced pressure for the infrared and Raman measurements.

d_8-Cyclopentanone (4)

This material was purchased from Merck, Sharpe, and Dohme (Canada) Ltd. and used as received.

The infrared spectra of the pure liquids and solutions were measured in a Perkin-Elmer Model 521 infrared spectrophotometer. The digitally recorded spectra were processed as described elsewhere (1, 11). The same operating conditions, spectral slit widths, and solvent ranges were used as for cyclohexanone (1).

The Raman spectra were obtained with the 4880 Å excitation of a Spectra-Physics induction ion laser and a Spex 1400 recording spectrometer. The samples were distilled into quartz capillary tubes and sealed under helium at a pressure of 100–200 Torr. Under these conditions good Raman spectra could be obtained and reliable polarization measurements could be made.[9] The infrared spectra are shown in Fig. 4, and the Raman spectra in Fig. 5. The positions of the peaks of both the infrared and Raman bands are listed in Table 4*a–d*. Averaged values of the infrared and Raman peak positions were used in the computations except for the C=O stretch bands for which infrared values were employed.

Discussion

Factors influencing the choice of the initial set of force constants have been discussed in connection with cyclohexanone (1). Theoretically there are 1128 quadratic force constants. An initial set of 16 diagonal and 60 off-diagonal constants was used. During the refinement many of the interaction constants were eliminated and a satisfactory force field was achieved with the 16 diagonal and 16 off-axis constants listed in Table 5. Initially the starting constants were transferred from literature data for acetone and the generalized alicyclic hydrocarbon as was done for cyclohexanone (1). Subsequently the refined values obtained for cyclohexanone were used as starting values for cyclopentanone. Both computations converged to a similar force field but convergence from the cyclohexanone input data was much faster and only these values will be reported.[10]

The same systematic trend towards the differentiation of the force constants associated with the α and β carbon atoms was observed as with cyclohexanone *viz*:

$$K_{d(\alpha)} > K_{d(\beta)}$$
$$K_{r(\alpha)} > K_{r(\beta,\gamma)}$$
$$H_{\gamma(\alpha)} < H_{\gamma(\beta)}$$
$$H_{\omega(\alpha)} > H_{\omega(\beta)}$$
$$H_{\delta(\alpha)} < H_{\delta(\beta)}$$
$$H_{\chi} > H_{\iota}$$
$$H_{\tau(\alpha)} < H_{(\beta,\gamma)}$$

The stretch constant ($K_{r(\beta,\gamma)}$) and the corresponding C—C torsion ($H_{\tau(\beta,\gamma)}$) (internal coordinates 14, 45) were kept fixed in the sense that values for the β and γ positions were not allowed to differ. All the interaction constants were kept fixed during the refinement. A total of 144 experimental frequencies, derived from the four isotopic species, were used to refine 15 adjustable diagonal force constants. The force constants associated with the alicyclic part of the molecule are all well determined, but force constant No. 12 (H_χ) proved to be strongly correlated with force constant No. 3 (K_ν) and had to be kept fixed during the refinement.

The analysis of the 36 normal modes is based on the potential energy distribution coefficients (E_p) and the normal vibrations are classified as GF, ZF, or DF (1). These are listed in Table 4*a–d* together with the observed and calculated frequency data. Only the four largest E_p coefficients are listed, and these only if they exceed unity. In the vibrational diagrams only motions associated with $E_p > 10$ are indicated.

The C—C—C Skeletal Vibrations

The six normal modes below 600 cm^{-1} are listed in Table 6; they can be traced through the isotopic series by the E_p coefficients. The lowest band is a ring pucker (τ_α, τ_β); it has been described as a pseudo-rotation of the ring (2, 12) and has been recently investigated in detail by Ikeda and Lord (8). We observe it in the Raman spectra of **1** and **2**. The next higher fundamental at 239 cm^{-1} in **1** is an out-of-plane ring distortion with symmetric twists of the β and γ C—C bonds (τ_β, τ_γ) and closure of the β CCC angles (ω_β). Bands III and IV of Table 6 involve deformations of the C_α—CO—C_α group (ρ, ε) and will be discussed with the carbonyl vibrations.

The two in-plane ring vibrations V and VI

[9]We wish to thank Dr. W. F. Murphy for making these measurements for us.

[10]The detailed numerical calculations for the refinement from the cyclohexanone input data will be found in ref. 10 where they are used as illustrative examples in the description of the computer programs.

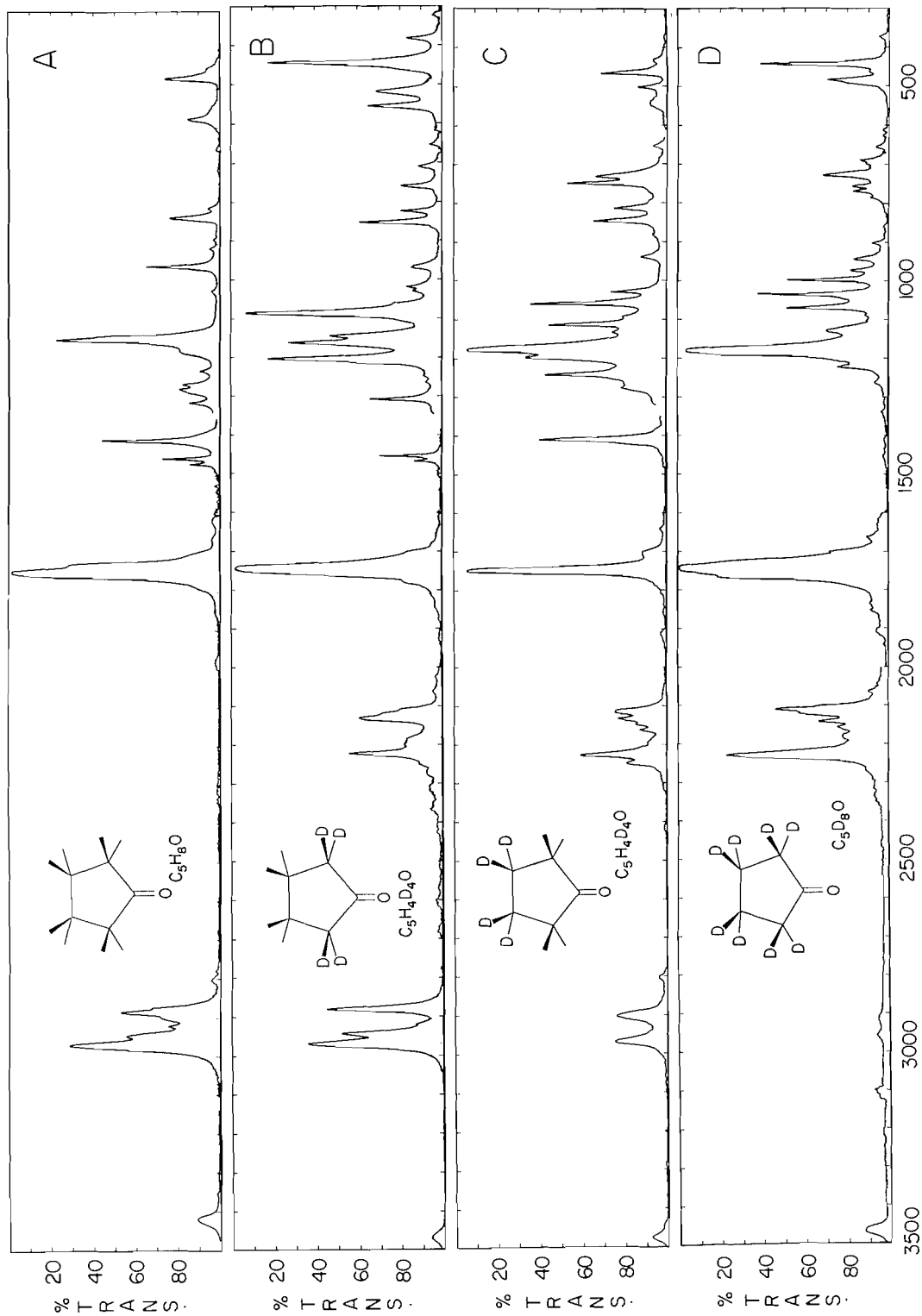

FIG. 4. Infrared spectra in solution. Solvent CCl_4 (4000–1380/630–240 cm^{-1}); CS_2 (1380–630 cm^{-1}). Path length 1 mm.

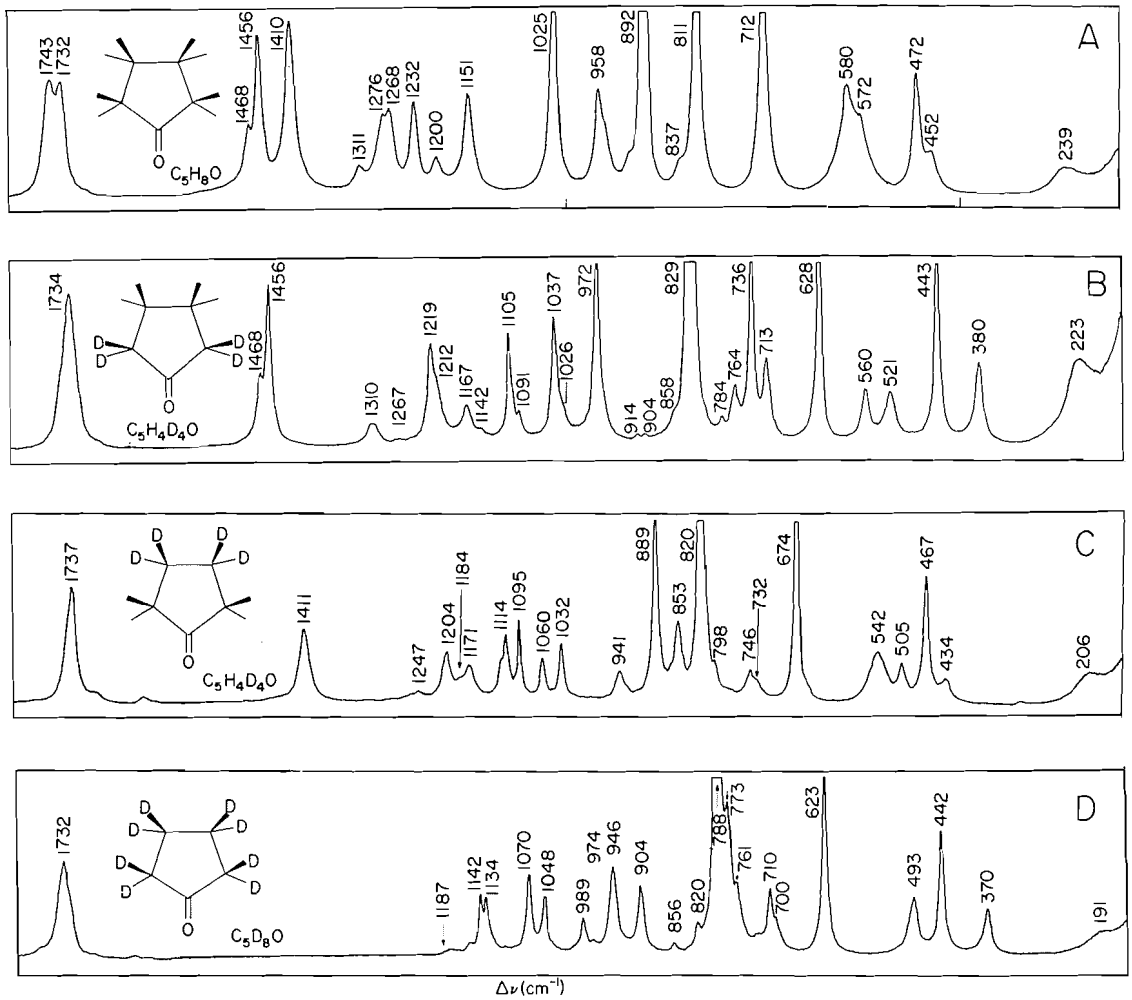

FIG. 5. Raman spectra of the pure liquids measured without polarizers; excitation with 4880 Å argon ion source. The region $\Delta\nu$ = 4600–1800 cm^{-1} is not shown, but the peak positions are listed in Table 12.

overlap near 570 cm^{-1} in **1** and near 490 cm^{-1} in **4**; they are well separated in **2** and **3**. The C_α—CO—C_α angle (χ) and the α C—C—C angle (ω_α) participate in V which is sensitive to α-deuteration. Both V and VI are highly delocalized. Mode VI emphasizes the effect of deuterium substitution on the mixing of the internal co-ordinates (Table 7*a*); on β-deuteration a large contribution to the energy of this mode is injected from the β D—C—C angle bend (γ_β). Above 600 cm^{-1} contributions from H—C—C and D—C—C bend motions predominate and the C—C stretch motions in this region are discussed with the C—H and C—D deformations.

The Carbonyl Group

Linear stretch of the C=O bond (v) contributes only about 80% to the mode energy of the "C=O stretching group vibration" (Table 8) and the remaining energy is localized mainly in the α C—C stretch (r_α) and the C_α—CO—C_α bend (χ). In **1** the position of the C=O stretch vibration is strongly affected by Fermi resonance.[11] This has not been considered in these calculations since the displacement effect is small, especially for the pure liquid. Of potentially greater significance is the large downward shift in the C=O stretch frequency in passing from

[11]See ref. 13 and other references cited therein.

TABLE 4. Vibrational analysis

(*a*) Cyclopentanone (**1**)

Band No.	Symmetry type	Wavenumber (cm^{-1}) Calculated	Observed Infrared	Observed Raman	Raman polarization	Potential energy distribution (E_p)				Mode type*
1	B	106	(105)†	95	—	37(τ_α)	35(τ_β)	12(ρ)	8(ω_α)	ZF
2	A	239	(240 w)†	239 w	0.76	51($\tau_{\beta,\gamma}$)	26(ω_β)	10(ω_α)	5(γ_β)	ZF
3	B	440	450 m‡	452 m	0.79	75(ρ)	10(γ_α)	4(τ_α)	4($\tau_{\beta,\gamma}$)	GF
4	B	478	471 vs	472 vs	0.83	75(ε)	7(r_β)	6(r_α)	2(ω_α)	GF
5	A	545	564 m‡	572 s	0.30	27(χ)	25(ω_α)	11($r_{\beta,\gamma}$)	11(ε)	DF
6	B	573	580 s	580 s	0.83	47(ω_β)	20(ω_α)	13(γ_β)	5(r_α)	DF
7	A	771	706 w	712 vs	0.03	66(r_α)	11(γ_α)	6(γ_β)	6(ω_α)	GF
8	A	832	806 m	811 vvs	0.07	61(γ_α)	13(γ_β)	10(r_α)	10($r_{\beta,\gamma}$)	ZF
9	B	832	831 s	837 w	d.p.	61(γ_β)	21(γ_α)	5(r_β)	4(r_α)	ZF
10	A	894	889 w	892 vvs	0.03	79($r_{\beta,\gamma}$)	7(γ_β)	7(γ_α)	3(ω_β)	GF
11	B	954	—	—	—	55(r_β)	22(γ_α)	6(γ_β)	6(ε)	ZF
12	B	974	958 vs	958 s	0.80	49(γ_α)	29(γ_β)	8(r_β)	3(ρ)	ZF
13	A	1038	1021 m	1025 vs	0.59	35(γ_α)	28($r_{\beta,\gamma}$)	24(γ_β)	2(ω_β)	DF
14	A	1066	—	—	—	41(γ_β)	32($r_{\beta,\gamma}$)	11(γ_α)	4(ω_α)	ZF
15	A	1149	1148 vvs	1151 s	0.70	66(γ_α)	30(γ_β)	5($r_{\beta,\gamma}$)	—	GF
16	B	1154	—	—	—	49(γ_α)	42(r_α)	7(ε)	3(r_β)	ZF
17	B	1174	1176 s	—	—	45(γ_α)	40(r_α)	9(ε)	8(γ_b)	ZF
18	A	1184	—	1200 m	0.6	68(γ_α)	26(γ_β)	19($r_{\beta,\gamma}$)	2(r_α)	GF
19	B	1211	1227 m	1232 s	0.79	84(γ_α)	21(r_β)	11(γ_β)	3(ε)	GF
20	B	1231	1262 s	1268 s	—	79(γ_β)	12(γ_α)	10(r_α)	1(r_β)	GF
21	A	1232	—	—	—	71(γ_β)	21(γ_α)	9($r_{\beta,\gamma}$)	2(r_α)	GF
22	A	1280	1274 s	1276 s	—	79(γ_β)	21($r_{\beta,\gamma}$)	18(γ_α)	2(δ_β)	GF
23	B	1327	1311 s	1311 m	0.77	91(γ_β)	8(γ_α)	6(r_β)	4(δ_α)	GF
24	A	1412	1409 vs	1410 vs	0.70	74(δ_α)	25(γ_α)	2(γ_β)	2(δ_β)	GF
25	B	1418	—	—	—	70(δ_α)	25(γ_α)	4(γ_β)	—	GF
26	A	1460	1454 vs	1456 vs	0.74	72(δ_β)	28(γ_β)	1(δ_α)	—	GF
27	B	1467	1469 s	1468 m	—	73(δ_β)	27(γ_β)	—	—	GF
28	A	1745	1748 vvs	1732 vs 1743 vs	0.3 0.4 §	78(v)	13(r_α)	5(χ)	2(ε)	GF
29	B	2884	2873 s	—	—	99(d_β)	—	—	—	GF
30	A	2885	2885 vs	2886 vs	—	99(d_β)	—	—	—	GF
31	B	2899	2898 s	2905 vs	—	99(d_α)	—	—	—	GF
32	A	2901	—	—	—	99(d_α)	—	—	—	GF
33	B	2952	2946 s	—	—	97(d_β)	3(d_α)	—	—	GF
34	A	2958	—	—	—	89(d_β)	11(d_α)	—	—	GF
35	B	2970	2969 vs	2972 vs	—	97(d_α)	3(d_β)	—	—	GF
36	A	2971	—	—	—	89(d_α)	11(d_β)	—	—	GF

*GF, group frequency; ZF, zone frequency; DF, delocalized frequency.
†These are new measurements on a Perkin–Elmer Model 180 spectrophotometer made after completion of the numerical analysis.
‡Inflection.
§Fermi resonance doublet.

(*b*) $\alpha\alpha\alpha'\alpha'$-$d_4$-Cyclopentanone (**2**)

Band No.	Symmetry type	Wavenumber (cm^{-1}) Calculated	Observed Infrared	Observed Raman	Raman polarization	Potential energy distribution (E_p)				Mode type*
1	B	96	(98)†	89	—	38(τ_α)	36(τ_β)	10(ρ)	8(ω_α)	ZF
2	A	222	—	223 m	—	50($\tau_{\beta,\gamma}$)	26(ω_β)	9(ω_α)	5(γ_β)	ZF
3	B	387	378 m	380 s	0.75	69(ρ)	21(γ_α)	3(ω_β)	2(τ_α)	GF
4	B	456	442 vs	443 vs	0.75	74(ε)	6(γ_α)	6(r_β)	5(γ_α)	GF
5	A	530	519 s	521 m	0.26	26(χ)	25(ω_α)	11(γ_α)	11(ε)	DF
6	B	560	557 s	560 m	0.73	43(ω_β)	20(ω_α)	13(γ_β)	6(γ_α)	DF

TABLE 4. (*Continued*)

(*b*) ααα′α′-d_4-Cyclopentanone (**2**)

Band No.	Symmetry type	Wavenumber (cm^{-1}) Calculated	Observed Infrared	Observed Raman	Raman polarization	Potential energy distribution (E_p)				Mode type*
7	A	666	624 vw	628 vvs	0.03	67(γ_α)	13(r_α)	8(γ_β)	3($r_{\beta,\gamma}$)	GF
8	A	704	710 s	713 s	0.58	38(γ_α)	35(r_α)	5(ω_α)	4(ω_β)	ZF
9	B	743	760 s	764 m	0.76	62(γ_α)	16(γ_β)	5(ρ)	5(ω_β)	ZF
10	A	787	—	736 s	0.16	80(γ_α)	13($r_{\beta,\gamma}$)	2(r_α)	—	GF
11	A	811	825 s	829 vvs	0.04	37(γ_α)	35($r_{\beta,\gamma}$)	12(r_α)	6(γ_β)	ZF
12	B	825	{853 vs	858 w‡	—	57(γ_α)	27(r_β)	3(ω_β)	3(γ_β)	ZF
13	B	873	} —	—	—	76(γ_α)	13(γ_β)	5(ρ)	1(r_α)	GF
14	B	901	—	904 vw	—	57(γ_β)	29(γ_α)	5(ρ)	2(r_β)	ZF
15	A	992	970 s	972 vs	0.60	45($r_{\beta,\gamma}$)	32(γ_α)	12(γ_β)	9(r_α)	ZF
16	B	1023	1020 s	1026 m*	—	78(δ_α)	23(γ_α)	5(r_β)	2(ω_α)	GF
17	A	1029	1031 s	1037 vs	0.49	62(δ_α)	21(γ_α)	11(γ_β)	4(r_α)	ZF
18	B	1063	1087 vvs	1091 m	—	40(r_β)	36(γ_α)	20(ε)	8(r_α)	ZF
19	A	1067	—	1105 vs	0.38	64(γ_β)	10($r_{\beta,\gamma}$)	10(γ_α)	10(δ_α)	ZF
20	A	1092	1145 vs	1142 w	—	67($r_{\beta,\gamma}$)	25(γ_α)	8(γ_β)	5(r_α)	GF
21	B	1166	1163 vvs	1167 m	0.83	77(r_α)	16(r_β)	9(γ_β)	9(γ_α)	GF
22	A	1219	1218 w‡	1219 vs	0.64	91(γ_β)	4($r_{\beta,\gamma}$)	3(γ_α)	2(r_α)	GF
23	B	1222	1204 vvs	1212 s‡	0.80	88(γ_β)	8(r_α)	2(γ_α)	—	GF
24	A	1269	1269 w	1267 vw	—	97(γ_β)	26($r_{\beta,\gamma}$)	2(δ_β)	1(ω_α)	GF
25§	B	1325	1309 s	1310 m	0.68	99(γ_b)	8(r_β)	1(δ_β)	1(r_α)	GF
26	A	1458	1454 s	1456 vs	—	74(δ_β)	29(γ_β)	—	—	GF
27	B	1467	1469 m	1468 s	0.80	73(δ_β)	27(γ_β)	—	—	GF
28	A	1743	1744 vvs	1734 vs	0.3	78(v)	13(r_α)	5(χ)	2(ε)	GF
29	B	2120	—	2126 s‡	—	97(d_α)	1(r_α)	—	—	GF
30	A	2124	2130 vs	2130 vs	—	97(d_α)	1($r_{\beta,\gamma}$)	—	—	GF
31	A	2215	—	2210 s‡	—	98(d_α)	1(γ_α)	—	—	GF
32	B	2217	2223 vs	2221 s	—	98(d_α)	1(γ_α)	—	—	GF
33	B	2884	{2881 vs	2879 vs	—	99(d_β)	—	—	—	GF
34	A	2885	} —	—	—	99(d_β)	—	—	—	GF
35	B	2952	2944 vs	2946 m‡	—	100(d_β)	—	—	—	GF
36	A	2959	2964 vs	2969 s	—	99(d_β)	—	—	—	GF

*GF, group frequency; ZF, zone frequency; DF, delocalized frequency.
†These are new measurements on a Perkin–Elmer Model 180 spectrophotometer made after completion of the numerical analysis.
‡Inflection.
§We have taken note of the anomaly in the Type B assignment of the Raman Band 25 which appears to be polarized.

(*c*) βββ′β-d_4-Cyclopentanone (**3**)

Band No.	Symmetry type	Wavenumber (cm^{-1}) Calculated	Observed Infrared	Observed Raman	Raman polarization	Potential energy distribution (E_p)				Mode type*
1	B	101	—	—	—	37(τ_α)	35(τ_β)	12(ρ)	8(ω_α)	ZF
2	A	203	—	206 m	—	50($\tau_{\beta,\gamma}$)	25(ω_β)	10(ω_α)	8(γ_β)	ZF
3	B	438	—	434 m	0.76	71(ρ)	10(γ_α)	5(ω_β)	4(τ_α)	GF
4	B	468	—	467 vs	0.73	71(ε)	8(r_β)	6(r_α)	2(ω_α)	GF
5	B	515	—	505 m	0.78	34(ω_β)	34(γ_β)	14(ω_α)	6(ρ)	ZF
6	A	532	—	542 m	0.19	26(χ)	23(ω_α)	12($r_{\beta,\gamma}$)	11(ε)	DF
7	B	688	731 s	732 w	d.p.	63(γ_β)	13(ω_β)	7(ω_α)	5(r_α)	ZF
8	A	716	—	674 vvs	0.04	43(γ_β)	25(r_α)	22(γ_α)	3(ω_β)	ZF
9	A	775	748 vs	746 m	0.40	56(γ_β)	15($r_{\beta,\gamma}$)	12(r_α)	5(ω_α)	ZF
10	A	807	813 s	820 vvs	0.06	33(r_α)	27($r_{\beta,\gamma}$)	15(γ_α)	10(γ_β)	DF
11	B	831	{ —	—	—	72(γ_β)	16(γ_α)	4(r_β)	2(ε)	GF
12	B	857	} 847 vs	853 s	0.80	42(γ_β)	27(r_β)	12(γ_α)	7(ε)	ZF

TABLE 4. (*Continued*)

(*c*) ββββ′β-d_4-Cyclopentanone (**3**)

Band No.	Symmetry type	Wavenumber (cm^{-1}) Calculated	Observed Infrared	Observed Raman	Raman polarization	Potential energy distribution (E_p)				Mode type*
13	A	877	883 w	889 vs	0.16	72(γ_β)	14($r_{\beta,\gamma}$)	2(χ)	2(γ_α)	GF
14	A	910	—	—	—	42(γ_β)	27($r_{\beta,\gamma}$)	15(γ_α)	6(r_α)	ZF
15	A	967	940 m	941 m	0.8	51(γ_α)	30(γ_β)	9($r_{\beta,\gamma}$)	3(ω_β)	ZF
16	B	994	1028 s	1032 s	0.86	58(γ_α)	25(γ_β)	5(ρ)	3(r_β)	ZF
17	A	1056	1058 vvs	1060 s	0.78	74(δ_β)	26(γ_β)	11($r_{\beta,\gamma}$)	3(γ_α)	GF
18	B	1063	—	—	—	74(δ_β)	23(γ_β)	6(r_β)	4(ω_β)	GF
19	B	1124	1113 vs	1114 s	0.84	57(γ_b)	45(r_β)	11(γ_α)	2(ω_β)	ZF
20	A	1130	1092 m	1095 vs	0.09	57(γ_α)	29($r_{\beta,\gamma}$)	16(γ_β)	3(δ_β)	ZF
21	B	1158	1177 vvs	1184 w	d.p.	53(r_α)	36(γ_α)	11(ε)	7(ω_α)	ZF
22	A	1172	—	1171 m	—	60($r_{\beta,\gamma}$)	42(γ_α)	18(γ_β)	2(ω_α)	ZF
23	B	1179	1196 vs	1204 s	0.83	50(γ_α)	40(r_α)	8(ε)	3(γ_β)	ZF
24	A	1217	—	—	—	86(γ_α)	10($r_{\beta,\gamma}$)	9(γ_β)	5(r_α)	GF
25	B	1218	1241 s	1247 vw	d.p.	100(γ_α)	9($r_{\beta,\gamma}$)	3(r_α)	1(ε)	GF
26	A	1412	1408 vs	1411 s	—	77(δ_α)	25(γ_α)	—	—	GF
27	B	1416	—	—	—	74(δ_α)	25(γ_α)	—	—	GF
28	A	1745	1744 vvs	1737 vs	—	78(v)	13(r_α)	5(χ)	2(ε)	GF
29	B	2107	2114 s	2111 vs	—	98(d_β)	1(r_β)	—	—	GF
30	A	2112	2131 s	2137 vs	—	97(d_β)	2($r_{\beta,\gamma}$)	—	—	GF
31	B	2200	2225 vs	2225 s	—	99(d_β)	1(γ_β)	—	—	GF
32	A	2218	2247 s	2252 m	—	97(d_β)	2(γ_β)	—	—	GF
33	B	2899	2901 s	2904 vs	—	99(d_α)	—	—	—	GF
34	A	2900	—	—	—	99(d_α)	—	—	—	GF
35	A	2969	2967 s	2968 s	—	100(d_α)	—	—	—	GF
36	B	2970	—	—	—	100(d_α)	—	—	—	GF

*GF, group frequency; ZF, zone frequency; DF, delocalized frequency.

(*d*) d_8-Cyclopentanone (**4**)

Band No.	Symmetry type	Wavenumber Calculated	Observed Infrared	Observed Raman	Raman polarization	Potential energy distribution (E_p)				Mode type*
1	B	93	—	—	—	38(τ_α)	36(τ_β)	10(ρ)	8(ω_α)	ZF
2	A	189	—	191 m	—	50($\tau_{\beta,\gamma}$)	25(ω_β)	9(ω_α)	8(γ_β)	ZF
3	B	384	368 m	370 s	0.74	65(ρ)	22(γ_α)	4(ω_β)	3(τ_α)	GF
4	B	450	438 vs	442 vs	0.70	72(ε)	7(r_β)	5(r_α)	5(γ_α)	GF
5	B	503	481 s	—	—	33(γ_β)	31(ω_β)	14(ω_α)	8(ρ)	DF
6	A	518	493 s†	493 s	0.55	25(χ)	24(ω_α)	12(γ_α)	10(ε)	DF
7	A	629	618 w	623 vs	0.04	55(γ_α)	23(γ_β)	9(r_α)	4($r_{\beta,\gamma}$)	ZF
8	B	668	689 m	700 m	—	47(γ_β)	16(γ_α)	15(ω_β)	7(ω_α)	DF
9	A	697	706 m†	710 s	0.33	38(r_α)	31(γ_α)	5(ω_α)	5(γ_β)	ZF
10	B	758	727 vs	—	d.p.	41(γ_α)	24(γ_β)	21($r_{\beta,\gamma}$)	2(ω_β)	ZF
11	B	766	756 s	761 m†	—	45(γ_β)	44(γ_α)	4(ρ)	1(r_β)	ZF
12	A	774	769 s	773 vs	—	45($r_{\beta,\gamma}$)	23(γ_α)	9(γ_β)	9(r_α)	ZF
13	A	781	785 m	788 vvs	0.04	68(γ_α)	12(γ_β)	6($r_{\beta,\gamma}$)	3(r_α)	GF
14	A	798	—	—	—	58(γ_β)	28(γ_α)	4($r_{\beta,\gamma}$)	2(r_α)	ZF
15	A	864	856 vw	856 w	p.	80(γ_β)	8(γ_α)	4($r_{\beta,\gamma}$)	1(δ_α)	GF
16	B	870	902 m	904 s	0.80	76(γ_α)	12(γ_β)	5(ρ)	—	GF
17	B	919	972 s	974 w	d.p.	56(γ_β)	29(γ_α)	5(ρ)	1(d_α)	ZF
18	A	945	942 s	946 vs	0.76	56(γ_β)	24(γ_α)	6($r_{\beta,\gamma}$)	3($\tau_{\beta,\gamma}$)	ZF
19	B	1019	996 vs	989 m	—	50(γ_α)	24(γ_β)	11(δ_α)	10(ε)	ZF
20	B	1024	1033 vs	—	—	66(δ_α)	26(γ_α)	12(r_β)	3(ε)	GF

TABLE 4 (*Concluded*)

(*d*) d_8-Cyclopentanone (**4**)

Band No.	Symmetry type	Wavenumber Calculated	Observed Infrared	Observed Raman	Raman polarization	Potential energy distribution (E_p)				Mode type*
21	A	1036	1044 s†	1048 s	0.54	71(δ_α)	23(γ_α)	10(r_α)	2(ω_α)	GF
22	B	1060	1067 vs	1070 vs	0.46	70(δ_β)	25(γ_β)	22($r_{\beta,\gamma}$)	4(γ_α)	GF
23	B	1066	—	—	—	73(δ_β)	23(γ_β)	4(ω_β)	4(r_β)	GF
24	A	1071	—	—	—	46(γ_α)	28($r_{\beta,\gamma}$)	12(r_α)	10(γ_β)	ZF
25	B	1129	1127 s	1134 s	—	57(γ_β)	45(r_β)	5(ε)	4(r_α)	ZF
26	A	1157	—	1142 s	p.	86($r_{\beta,\gamma}$)	41(γ_β)	3(ω_α)	1(γ_α)	GF
27	B	1167	1181 vvs	1187 vw	d.p.	90(r_α)	11(r_β)	11(ε)	8(γ_α)	GF
28	A	1743	1742 vs	1732 vs	—	78(v)	13(r_α)	5(χ)	2(ε)	GF
29	B	2107	2110 vs	2099 m	—	97(d_β)	1(r_β)	—	—	GF
30	A	2111	—	—	—	90(d_β)	7(d_α)	2($r_{\beta,\gamma}$)	—	GF
31	B	2119	2119 s†	2120	—	97(d_α)	1(r_α)	—	—	GF
32	A	2125	—	—	—	90(d_α)	7(d_β)	1($r_{\beta,\gamma}$)	—	GF
33	B	2198	2181 s	2181 m	—	87(d_β)	12(d_α)	—	—	GF
34	A	2206	—	—	—	56(d_α)	43(d_β)	—	—	ZF
35	B	2219	2229 vs	2231 vs	—	86(d_α)	12(d_β)	1(γ_α)	—	GF
36	A	2227	—	—	—	54(d_β)	43(d_α)	2(γ_β)	1(γ_α)	ZF

*GF, group frequency; ZF, zone frequency; DF, delocalized frequency.
†Inflection.

the vapor to the liquid state (~30 cm^{-1}). The liquid state values were used in this work.[12]

The in-plane C=O deformation (ε) is easily identified as a strong band in both the infrared and Raman spectra at 471, 456, 467, and 442 cm^{-1} in **1**–**4** respectively. It is highly localized with E_p 71–75. The out-of-plane C=O vibration (ρ) is the lowest of the three carbonyl frequencies at 451, 379, 434, 369 cm^{-1}; it is a medium-strong depolarized Raman band, strongly affected by α-deuteration, and in all four isotopic species accounts for 65–75% of the mode energy. This contrasts with cyclohexanone in which it is highly delocalized.

Bending Vibrations Involving CH and CD Bonds

There are 21 normal vibrations between 600 and 1500 cm^{-1} that involve HCH, HCC, DCD, and DCC angle deformations. Rigorous classification of these as methylene wag, twist, or rock vibrations is impractical since the normal modes are too complex and many couple strongly with C—C stretch co-ordinates.

The CH_2 scissors motions are all good group frequencies (E_p 70–77) with the residual energy localized mainly in the rock/twist motions on the same carbon atom. For the CD_2 scissor the E_p range is 62–74 which brings one of them down into the marginal group frequency range ($E_p < 66$).[13] At each of the C_α and C_β atoms the scissors motion may be in-phase or out-of-phase with its partner across the ring. The calculated wavenumber differences between such pairs are in the range 4–12 cm^{-1} but not all are separated in the measured spectra (Table 9). The empirically well known displacement of the C_α methylene motion to lower wavenumber is confirmed by the calculations. The corresponding effect on the $H_{\gamma(\alpha)}$ force constant has been noted (see Discussion section). Only a few of the other methylene deformation motions can be clearly identified as rocks, wags, or twists[14] (Table 10).

[12]In one computation the observed "carbonyl stretch" frequency was changed to a vapor phase value of 1771 cm^{-1} for all four species with all other experimental frequencies and all input force constants unchanged. Only three of the refined force constants were altered (Table 5), and these were marginal except for the C=O stretch; there were no significant changes in the E_p coefficients (Table 8). It follows that the vibrational modes are not substantially affected by the use of the condensed state experimental frequencies and even less so by the much smaller Fermi resonance displacement in **1**.

[13]This is band 17 in **2** (Fig. 4*b*).

[14]The differentiation between a wag and a twist or between a scissor and a rock depends on the relative signs of the appropriate eigenvectors. These are not included in Table 4*a*–*d* but are recorded in the eigenvector matrices which are listed in ref. 10.

TABLE 5. Valence force constants*

No.	Symbolic description*	Co-ordinates involved	Common atoms	Starting value†	Refined value‡
		Stretch			
1	$K_{d(\alpha)}$	C—H	—	4.685	4.694
2	$K_{d(\beta)}$	C—H	—	4.610	4.645
3	K_{v}	C=O	—	9.652	10.149 (10.546)
4	$K_{r(\alpha)}$	C—C	—	4.564	4.252
5	$K_{r(\beta,\gamma)}$	C—C	—	4.186	4.144
		Bend			
6	$H_{\delta(\alpha)}$	∠HCH	—	0.554	0.495
7	$H_{\delta(\beta)}$	∠HCH	—	0.567	0.520
8	$H_{\gamma(\alpha)}$	∠HCC	—	0.628	0.601
9	$H_{\gamma(\beta)}$	∠HCC	—	0.657	0.677
10	$H_{\omega(\alpha)}$	∠CCC	—	1.068	1.012 (1.000)
11	$H_{\omega(\beta)}$	∠CCC	—	1.024	0.878 (0.882)
12	H_{χ}	∠CCC	—	1.111	1.111
13	H_{ε}	∠CCO	—	0.919	0.905
14	H_{ρ}	∠C—CO—C	—	0.534	0.341
15	$H_{\tau(\alpha)}$	∠CC—CC	—	0.008	0.032
16	$H_{\tau(\beta,\gamma)}$	∠CC—CC	—	0.093	0.089
		Interaction Constants *Stretch–Stretch*			
17	$F_{d,d}$	C—H, C—H	C	0.006	0.006
18	$F_{i,r(\alpha)}$	C=O, C—C	C	0.0	0.0
19	$F_{r,r}$	C—C, C—C	C	0.101	0.101
		Stretch–Bend			
20	$F_{v,\chi}$	C=O, ∠CCC	C	0.0	0.0
21	$F_{r,\gamma}$	C—C, ∠HCC	C—C	0.328	0.328
22	$F_{r,\gamma}$	C—C, ∠HCC	C	0.079	0.079
23	$F_{r,\omega}$	C—C, ∠CCC	C—C	0.417	0.417
24	$F_{r(\alpha),\chi}$	C—C, ∠CCC	C—C	0.417	0.417
25	$F_{r(\alpha),\varepsilon}$	C—C, ∠CCO	C—C	0.417	0.417
		Bend–Bend			
26	$F_{\gamma,\gamma}$	∠HCC, ∠HCC	C—C	−0.021	−0.021
27	$F_{\gamma,\omega}$	∠HCC, ∠CCC	C—C	−0.031	−0.031
28	$F_{\gamma,\gamma}^{qt}$	∠HCC, ∠HCC	C—C	0.0	0.0
29	$F_{\gamma,\gamma}^{qg}$	∠HCC, ∠HCC	C—C	0.0	0.0
30	$F_{\gamma,\gamma}^{qc}$	∠HCC, ∠HCC	C—C	0.0	0.0
31	$F_{\omega,\omega}$	∠CCC, ∠CCC	C—C	0.0	0.0
32	$F_{\omega,\chi}$	∠CCC, ∠CCC	C—C	0.0	0.0

*The force constant units and symbolism are described in ref. 1. The superscripts on the bend–bend interaction constants are qt (quasi *trans*), qg (quasi *gauche*), qc (quasi *cis*).
†The initial values for the force constants were taken from the refined force field established for cyclohexanone (see Table 3 of ref. 1).
‡The values in parentheses are obtained if an observed C=O stretch frequency of 1771 cm^{-1} is used, corresponding to a vapor state measurement. No other force constants change significantly.

C—C Stretch Vibrations

The bands identifiable as C—C in-plane stretch group frequencies are listed in Table 11. Most notable are the 1166 cm^{-1} (calcd) band in **2** and the bands at 1167 and 1157 cm^{-1} (calcd) in **4**. These motions are illustrated in **7–9** respectively. The intense band at 891 cm^{-1} in **1** is strongly polarized in the Raman spectrum and has been attributed to a ring breathing motion (2) and the E_ρ coefficients support this (Table 7*b*). However, in the deuterated species the "corresponding" bands as judged by the Raman intensity and polarization are readily assigned at 827, 817, 787 cm^{-1} in **2–4** respectively, but the E_ρ data in Table 7*b* suggest that with α-deuteration the energy in the $r_{\beta,\gamma}$ co-ordinate is greatly reduced and much of it transferred to the γ_α and γ_β angle bends. If this is so these modes can no longer be classified as ring breathing motions in **3** and **4** where the $r_{\beta,\gamma}$

TABLE 6. Vibrational modes below 600 cm^{-1}*

Ring vibration	Symmetry type	Isotopic species 1	2	3	4	Approximate description
I	B	106 (95)	96 (89)	101 (—)	93 (—)	Pseudo-rotation
II	A	239 (239)	222 (223)	203 (206)	189 (191)	Ring torsion
III	B	440 (451)	387 (379)	438 (434)	384 (369)	C=O out of-plane bend
IV	B	478 (472)	456 (443)	468 (467)	450 (440)	C=O in-plane bend
V	A	545 (568)	530 (520)	532 (542)	518 (493)	Sym. ring mode
VI	B	573 (580)	560 (559)	515 (505)	503 (481)	Asym. ring mode

*ν_{calcd} is given first followed by ν_{obs} in parentheses; the observed postions are the mean of the infrared and Raman measurements. Ring vibrations are as follows:

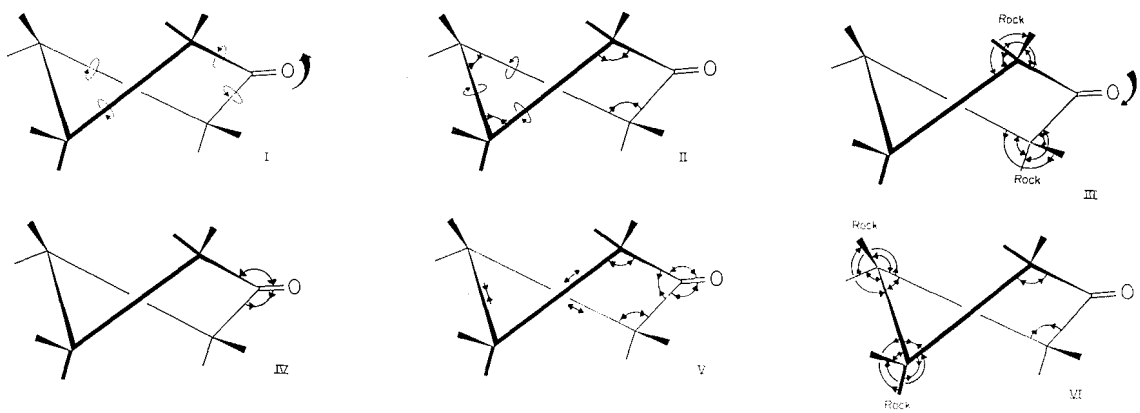

co-ordinates contribute less than 30% of the mode energy. One must bear in mind however that it is in this 800–1100 cm^{-1} region that the computations are most sensitive to small changes in the force field and over-simplified normal co-ordinate analyses are most prone to error.

C—H and C—D Stretch Vibrations

There are 8 calculated frequencies for each isotopic species in the C—H, C—D stretching region (Table 12). The wavenumber differences (1–8 cm^{-1}) calculated for the pairs of in-phase and out-of-phase motions at the C_α and C_β positions correlate with bands in the observed spectra and are reflected in the corresponding force constants. The C—H stretch modes are all

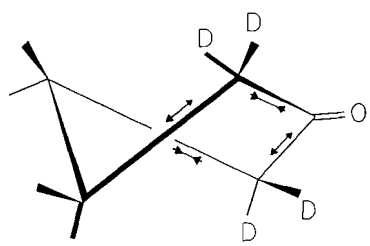

7

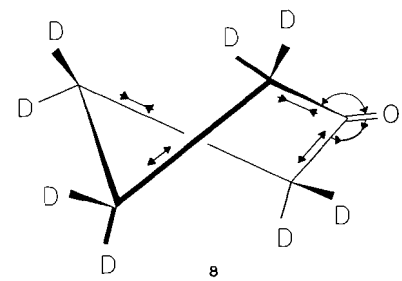

8

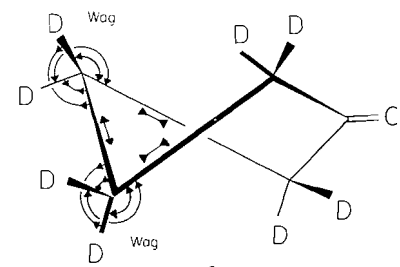

9

good group frequencies with over 90% of the potential energy localized in the C—H bonds. This is true also of most of the corresponding C—D modes except for the symmetric C—D

TABLE 7. Effect of isotopic substitution on the potential energy distribution

(*a*) In-plane ring mode (VI of Table 6)

Structure	Observed Raman wavenumber (cm^{-1})	Depolarization ratio	Potential energy distribution (E_p)		
			(ω_β)	(ω_α)	(γ_β)
1	580	0.83	47	20	13
2	560	0.73	43	20	13
3	505	0.78	34	14	34
4	481*	—	31	14	33

*Infrared band position.

(*b*) "Ring breathing" mode*

Structure†	Observed Raman wavenumber (cm^{-1})	Depolarization ratio	Potential energy distribution (E_p)			
			($r_{\beta,\gamma}$)	(γ_β)	(γ_α)	(r_α)
1	892	0.03	79	7	7	1
2	829	0.04	35	6	37	12
3	820	0.06	27	10	15	33
4	788	0.04	6	12	68	3

*Only motions associated with internal co-ordinates for which $E_p \geqslant 10$ are shown in the diagrams. The terms "Ψ-wag" etc. indicate that the eigenvectors associated with some of the C—D deformations are near zero; these are indicated as ‖‖ in the diagrams. This may not be significant within the error limits of the calculations.

†Ring vibrations as follows:

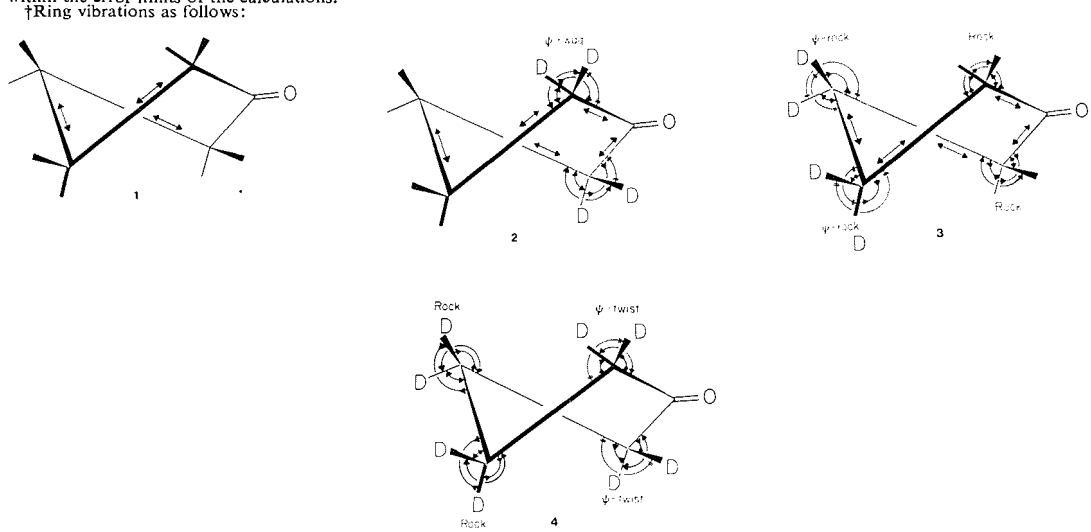

stretch in **4** where there is appreciable coupling between the C_α and C_β atoms.

Concluding Remarks

One may anticipate that these empirical force fields for cyclohexanone and cyclopentanone should aid in setting up similar computations on more complex molecules such as the β-decalones (with and without methyl substituents at the ring junctions) and the corresponding hydrindanones which would be closer analogs of steroids and other cyclic terpenoids. The replacement of C=O by N—H would open a route via piperidine and pyrrolidine to a set of potentially transferable force field parameters applicable to related *N*-heterocyclic systems. As a wider variety of molecular structures is investigated one may expect that a body of practical lore will evolve based on the co-ordination of the work of the various investigators who are taking this approach (14–16). At an earlier period most of the characteristic vibrational group frequencies of complex mole-

TABLE 8. Potential energy distributions associated with "C=O stretch" mode

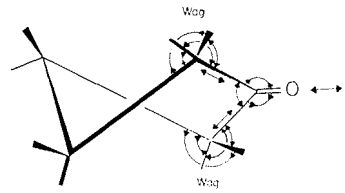

Phase	Structure	Infrared frequency (cm^{-1}) Calcd	Observed	Potential energy distribution (E_p) (v)	(γ_α)	(χ)	(γ_α)	(ε)
Liquid	**1**	1745	1748	78	13	5	5	2
	2	1743	1744					
	3	1745	1744					
	4	1743	1742					
Vapor*	**1**	1771	1771	79	12	5	2	2
	2							
	3							
	4							

*The vapor phase computations were obtained by using the measured vapor phase band position of **1** for all four isotopic species; no other observed band positions were changed. The same starting values for all the force constants were used (Table 5, column v). The following differences were observed in the refined force constants (*cf.* Table 5, column vi): K_v 10.546, $H_{\omega(\alpha)}$ 1.000, $H_{\omega(\beta)}$ 0.878 (mdyn Å^{-1}).

TABLE 9. Methylene scissor modes*

Structure	Wavenumber (cm^{-1}) asym C_β	sym C_β	asym C_α	sym C_α
1	1467 (1468)	1460 (1455)	1418 (1410)	1412 (1410)
2	1467 (1468)	1458 (1455)	1023 (1023)	1029 (1034)
3	1063 (1059)	1056 (1059)	1416 (1410)	1412 (1410)
4	1066 (1068)	1060 (1068)	1024 (1033)	1036 (1046)

*ν_{calcd} is given first followed by ν_{obs} averaged for infrared and Raman in parentheses.

cules were established in just such a fashion and, in many cases, it was only later that these were rationalized in terms of more formal vibrational theory. In retrospect the sequence of these events tends to be forgotten.

Molecular spectroscopists who are conditioned to the elegant vibrational analysis that can be made for small molecules of high symmetry may be disconcerted by such drastic simplification of the force fields, but this situation is not uncommon when theoretical concepts developed on the basis of simpler model systems are extended to a more general body of scientific data. The caution which must be exercised in applying normal co-ordinate analysis to polymers has been aptly summarized in eight aphorisms by Zerbi[15] and these are also relevant to molecules of the type considered here.

[15]See ref. 16, pp. 223–224.

TABLE 10. Vibrational modes assignable as methylene rock, wag, or twist group frequencies (cm^{-1})*

Structure	ν_{calcd}	ν_{obs}†	E_p	Approximate description‡
1	1327	1311	91(γ_β)	β CH_2 wag (o.o.p.)
	1280	1275	79(γ_β)	β CH_2 wag (i.p.)
	1232 }	1265	71(γ_β)	β CH_2 twist (i.p.)
	1231 }		79(γ_β)	β CH_2 twist (o.o.p.)
	1211	1232	84(γ_α)	α CH_2 wag (o.o.p.)
2	1325	1310	99(γ_β)	β CH_2 wag (o.o.p.)
	1269	1268	97(γ_β)	β CH_2 wag (i.p.)
	1222	1208	88(γ_β)	β CH_2 twist (o.o.p.)
	1219	1219	91(γ_β)	β CH_2 twist (i.p.)
	873	853	76(γ_α)	α CD_2 twist (o.o.p.)
	787	736	80(γ_α)	α CD_2 twist (i.p.)
	666	626	67(γ_α)	α CD_2 rock (i.p.)
3	1218	1244	100(γ_α)	α CD_2 wag (o.o.p.)
	877	886	72(γ_β)	β CD_2 twist (i.p.)
	831	849	72(γ_β)	β CD_2 twist (o.o.p.)
4	870	903	76(γ_α)	α CD_2 twist (o.o.p.)
	864	856	80(γ_β)	β CD_2 twist (i.p.)

*By our definition a group frequency must have at least 66% of the potential energy localized in the assigned internal co-ordinates (ref. 2).
†Average of the infrared and Raman band positions.
‡o.o.p. = out-of-phase; i.p. = in-phase.

TABLE 11. In-plane C—C stretch modes

Structure	ν_{calcd}	ν_{obs}(i.r.)	Potential energy distribution				ΣE_p
1	894*	889	79($r_{\beta,\gamma}$)	7(γ_β)	7(γ_α)	3(ω_β)	96
	771	706	66(r_α)	11(γ_α)	6(γ_β)	6(ω_α)	89
2	1166†	1163	77(r_α)	16($r_{\beta,\gamma}$)	9(γ_β)	9(γ_α)	111
	1092	1145	67($r_{\beta,\gamma}$)	25(γ_α)	8(γ_β)	5(r_α)	105
3	—	—					
4	1167†	1181	90(r_α)	11($r_{\beta,\gamma}$)	11(ε)	8(γ_α)	120
	1157†	1142‡	86($r_{\beta,\gamma}$)	41(γ_β)	11(ε)	8(γ_α)	145

*For diagram of this vibration see Table 7.
†Note that for these bands ΣE_p is appreciably greater than 100. This must be taken into account in assessing the relevance of the vibrational analysis.
‡This is the Raman peak position; the band was not observed in the infrared spectrum.

TABLE 12. C—H and C—D stretch group frequencies*

	Wavenumber (cm^{-1})							
	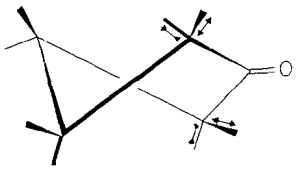		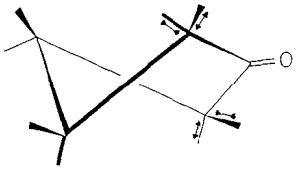		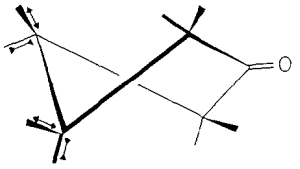		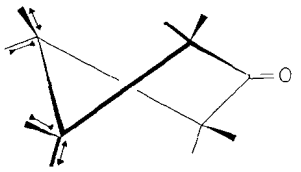	
	asym C_α i.p.		asym C_α o.o.p.		asym C_β i.p.		asym C_β o.o.p.	
Structure	Calcd.	Obsd.	Calcd.	Obsd.	Calcd.	Obsd.	Calcd.	Obsd.
1	2971	2971	2970	2971	2958	2946	2952	2946
2	2215	2210	2217	2222	2959	2966	2952	2945
3	2969	2968	2970	2968	2218	2249	2200	2225
4	2206	2181†	2219	2230	2227	2230†	2198	2181

	Wavenumber (cm^{-1})							
	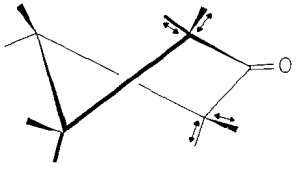		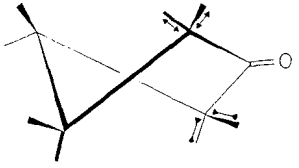		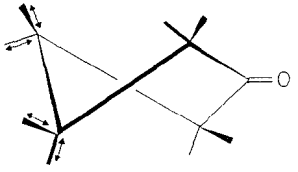		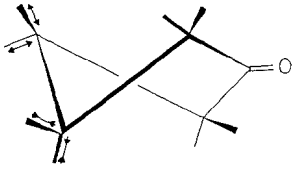	
	sym C_α i.p.		sym C_α o.o.p.		sym C_β i.p.		sym C_β o.o.p.	
Structure	Calcd.	Obsd.	Calcd.	Obsd.	Calcd.	Obsd.	Calcd.	Obsd.
1	2901	2901	2899	2901	2885	2886	2884	2873
2	2124	2130	2120	2126	2885	2880	2884	2880
3	2901	2902	2899	2902	2112	2134	2107	2110
4	2125	2120	2120	2120	2111	2110	2107	2110

*The observed positions are the mean of the infrared and Raman measurements. Asym (antisymmetric) and sym (symmetric) refer to the local site symmetry. o.o.p. = out-of-phase; i.p. = in-phase.
†These two modes are appreciably coupled.

We wish to thank Dr. L. C. Leitch for advice and assistance with the preparation of the deuterated compounds, and Dr. K. G. Kidd for comment and discussion during the preparation of the manuscript. We are also indebted to Professor G. W. King and Dr. H. E. Howard-Lock of McMaster University who provided us with an advanced copy of their publication and with whom we exchanged information during the course of the work. Our thanks are also due to Mrs. M. A. MacKenzie and Mr. A. Nadeau for their skilful technical help with the measurement of the spectra.

1. H. FUHRER, V. B. KARTHA, P. J. KRUEGER, H. H. MANTSCH, and R. N. JONES. Chem. Rev. **72**, 439 (1972).
2. H. E. HOWARD-LOCK and G. W. KING. J. Mol. Spectrosc. **35**, 393 (1970).
3. G. ERLANDSSON. J. Chem. Phys. **22**, 563 (1954).
4. J. H. BURKHALTER. J. Chem. Phys. **23**, 1172 (1955).
5. G. ERLANDSSON. Arkiv för Fysik, **9**, 399 (1955).
6. P. G. KÖKERITZ and H. SELÉN. Arkiv för Fysik, **16**, 197 (1959).
7. H. KIM and W. D. GWINN. J. Chem. Phys. **51**, 1815 (1969).
8. T. IKEDA and R. C. LORD. J. Chem. Phys. **56**, 4450 (1972).
9. H. J. GEISE and F. C. MIJLHOFF. Rec. Trav. Chim. Pays. Bas. **90**, 577 (1971).
10. H. FUHRER, V. B. KARTHA, K. G. KIDD, H. H. MANTSCH, and R. N. JONES. NRCC Bulletin No. 15. In preparation.
11. R. N. JONES. Pure and Appl. Chem. **18**, 303 (1969).
12. L. A. CARRIERA and R. C. LORD. J. Chem. Phys. **51**, 1815 (1969).
13. R. CATALIOTTI and R. N. JONES. Spectrochim. Acta, **27A**, 2011 (1971).
14. S. CALIFANO. Pure and Appl. Chem. **18**, 353 (1969).
15. T. SHIMANOUCHI. *In* Physical chemistry, an advanced treatise. Vol. IV. *Edited by* H. Eyring, D. Henderson, and W. Jost. Academic Press, New York. 1970. Chapt. 6.
16. G. ZERBI. Appl. Spectrosc. Rev. **2**, 193 (1969).